**V. G. Martynenko**
**Yu. N. Ulianov**, Cand. Sc. (Engineering)

National Technical University 'Kharkiv Polytechnic Institute', Kharkiv, Ukraine
e-mail: gradedegree@gmail.com
martynenko.volodymyr@gmail.com

**Keywords**: *anisotropic viscoelasticity, composite material, experimental investigation, elevated temperature, relaxation curve.*

UDC 620.172.251.226 / 620.172.251.282

# MODERNIZATION OF AN EXPERIMENTAL INSTALLATION AND A PROCEDURE FOR INVESTIGATING THE ANISOTROPIC VISCOELASTIC PROPERTIES OF COMPOSITE MATERIALS AT ELEVATED TEMPERATURES

*The paper describes the process of modernizing the existing installation designed for performing long-term tests of steel and aluminum cylindrical specimens for high-temperature creep. The modernization allowed conducting experimental studies of the anisotropic strength and viscoelastic characteristics of planar composite specimens at elevated temperatures. In order to reach the objective set, a scheme for reconstructing the specimen holders in the experimental installation was proposed, as well as the method of fixing them in the installation. The developed, designed and built automatic temperature control block for the electric furnace allowed maintaining elevated temperature with a sufficiently small error during its long use and controlling the heating temperature in a given range, which was necessary for studying the mechanical properties of composite specimens, as well as regulating the heating temperature in a given range. Conducting the experimental study of the instantaneous and long-term mechanical properties demonstrated the effectiveness of the improvements made for the experimental installation, as applied to the realization of such experiments.*

## Introduction

Fiber-reinforced polymeric composite materials (FRPCM) are used in automobile, aerospace, and heavy industries as well as in general consumer goods production [1, 2].

During operation, composite elements of structures and installations are subjected to the influence of elevated temperatures and high levels of stress. Since they are usually thin-walled elements, in order to maintain their performance, it is important to accurately calculate their behavior under the influence of variable temperatures and high loads [3–5].

Thus, the study of the mechanical properties of composite materials is an actual task at the moment, as modeling the mechanical behavior and determining the strength of the composite elements of installations is extremely important in their design.

Due to the presence of directed reinforcing fibers, the mechanical properties of composite materials are anisotropic. Furthermore, the properties of the polymer matrix of FRPCM are very sensitive to temperature changes [6], especially when passing through the glass transition temperature – a temperature value, above which a polymer changes its microstructure and the shape of its molecules becomes mobile under the influence of external loads [7]. This leads to the appearance of both the effect of elasticity (i.e., a linear change of body strains under the influence of loads due to changes in intermolecular distances) and the phenomenon of viscoelasticity – the process of strain growth over time under constant stresses and stress relaxation over time under constant strains [8]. Linear viscoelasticity is characterized by an integral proportionality between stresses and strains, and is also a reversible process – when loads are removed, the viscoelastic strains will return to the initial level over time [9].

The experimental investigation of quasi-static viscoelastic properties was performed for the planar load of a satin fabric carbon/epoxy composite in [10], for the interlaminar shear modulus of laminated composites in [11], for Prony series moduli and relaxation times as well as the temperature shift function of epoxy compounds in [12], for the creep properties of an epoxy adhesive in [13], for the planar orthotropic viscoelastic properties of a glass fabric composite at elevated temperatures in [14], for the viscoelastic compression parameters of filled rubber in [15], for the dependency of the reinforcement of exfoliated graphene oxide nanoplatelets on the mechanical and viscoelastic properties of natural rubber in [16], for the isotropic viscoelastic response of the woven composite in [17]. In [18] volumetric experiments on the viscoelasticity of an adhesive between composite and metal elements were provided. In [19] the viscoelasticity analysis and the experimental validation of anisotropic composite overwrap cylinders allowed the authors to adequately model such type of systems.

Therefore, the investigation of anisotropic viscoelastic properties of FRPCM is a complex engineering problem. Its solution requires that, firstly, stretch experiments be performed on composite specimens cut in different directions, their number depending on the degree of anisotropy of the mechanical properties; secondly, the specimens be fixed in the experimental installation properly in order to avoid undesirable deformations in holders; thirdly, the specimens be heated by a homogeneous and time-invariant temperature field, and, fourthly, viscoelastic deformations be measured accurately over a sufficiently long period of time.

Thus, at present, the development of an experimental equipment and the study of anisotropic viscoelastic properties of FRPCM at elevated temperatures is an actual engineering and scientific task.

**1. Description of the AIMA 5-2 experimental installation**

Fig. 1 presents the schematic diagram of the AIMA-5-2 experimental installation, that was used for conducting the experiment.

For the initial design of the installation the test specimen 12 is fixed with threaded ends in the grippers 3 and 11. The lower gripper 3 is connected to the upper part of the power screw 2 of the power reducer.

When disengaged, the power reducer is manually rotated by the hand-wheel 1, which is necessary when installing a specimen or quickly unloading specimens, for example, during a prolonged voltage de-energizing and specimen cooling.

While the worm-wheel of the power reducer is being rotated, the lead screw 2 moves up and down. The movement of the screw within 70 mm is limited by the limit switch. The upper gripper 11 is connected to the ball-joint suspension, which is the final link of the three-lever loading device consisting of the power lever 5, intermediate lever 7, and the weight lever 10. The levers are connected with each other by means of earrings 6. The weight lever 10 has the load holder 9 attached to it, which is necessary for the operation of the lever system with the arm ratio of 1:100. The weight lever is connected to the horizontal pointer of the levers 4, which is located on the face side of the installation. The total gear ratio of the lever system is 100:1 (the power lever is 8:1, the intermediate lever is 5:1, and the weight lever is 2.5:1). Each of the levers is balanced by its counterweight. The test specimen is placed in the electric furnace 13, providing the required test temperature.

The installation allows the testing of specimens in the load range from 50 to 400 N in the direct loading mode. In this case, a special traction with a gripper is attached to the lower end of the specimen.

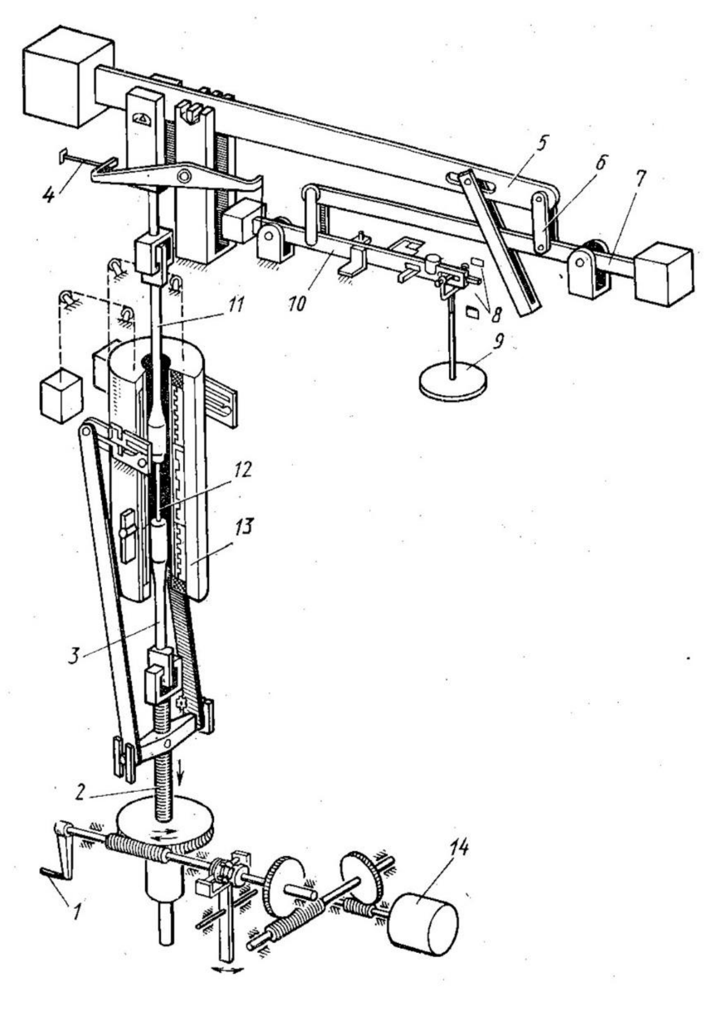


*Fig. 1. Schematic diagram of the AIMA-5-2 experimental installation [20]*

**2. Preparation of specimens for conducting the experiment**

The composite material under consideration is a combination of epoxy resin and long E-glass directed fibers [21, 22]. The orthogonal weaving scheme of the material provides high strength properties of thin shells made of this material, which are subjected to stretching or bending forces while preserving its light weight (approximately one-quarter of the analogous value for steel). At the same time, this composite material is not so strong as carbon fiber-reinforced polymer due to the weaker mechanical properties of glass fibers, but it is much cheaper owing to the lower price of their production in comparison with that of carbon fibers.

The generalized mechanical properties of epoxy resin and E-glass fibers are presented in papers [23–24] and [25–26], respectively.

Fig. 2 shows workpiece forms for producing specimens from glass-fiber reinforced plastic. Fig. 2, a shows the cutting scheme for producing experimental specimens presented in Fig. 2, b. Thus, each row of specimens was cut in its own direction from one large plate.

The polymer nature of epoxy resin matrix causes the appearance of the phenomenon of viscoelasticity [27]. The viscoelastic properties of FRPCM are not so noticeable at room temperature during the observable periods of time, but a relatively small increase in temperature up to 100°C shortens these periods to days, hours and even minutes.

Thus, the experiments on the viscoelastic properties of FRPCM need to be conducted at elevated temperatures, which needs to be maintained for a long period of time.

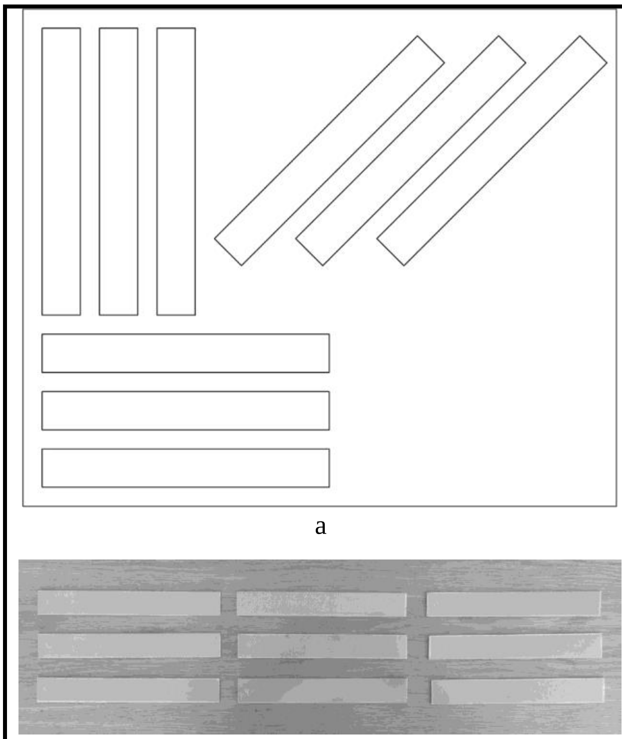

a

b

***Fig. 2. Glass fiber reinforced composite material:***
a – cutting scheme; b – cutout specimen workpieces

The preparation of specimens was performed according to the standard of the American Society for Testing and Materials D618 [28]. The procedure A was chosen as an adequate kind of preparation for the current testing purposes.

The geometry of the specimens was designed according to ASTM D638 standard [29]. Fig. 3 illustrates 2 mm thick ready-made specimens.

The specimens contain holes with diameters of 4 mm at their ends in order to provide their assembling in the testing installation. After the assembly, the ends of the specimens were tightened by the grippers in order to avoid the stress concentrations around the holes and provide the full fixation of the specimen ends.

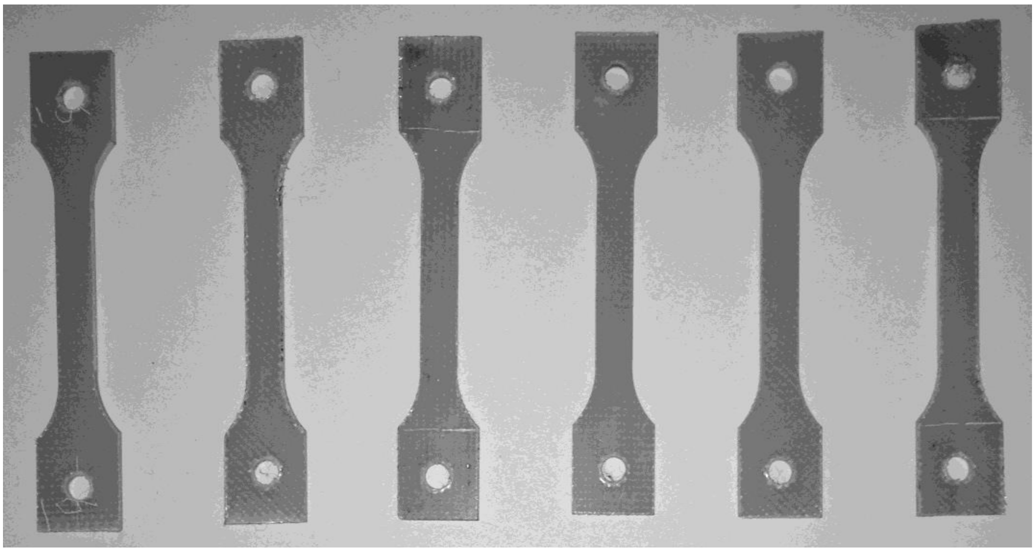

***Fig. 3. Experimental specimens***

**3. Modernization of the mechanical part of the experimental installation**

The AIMA 5-2 experimental installation was developed for testing cylindrical metal specimens, meant to be fastened with threaded connections. To study the mechanical properties of the composite material, it was necessary to develop a fasteners for flat specimens, which would ensure the pinching of their ends. Such fasteners were developed on the basis of steel cylindrical specimens with threaded ends. Figure 4 illustrates the process of assembling flat composite specimens in modernized grippers.

First, a specimen will be fixed in the initial position by means of both the holes at its ends and the pins on the halves of the grippers, as shown in Fig. 4, a. Then the other halves of the threaded fasteners will be put on the pins, as shown in Fig. 4, b. Finally, a measuring frame will be attached to the thread from two ends of the specimen, the other ends of the frame containing indicating gauges that must measure the relative movement of the grippers. The measuring frame will be tightened on the specimen ends, using four bolts and nuts, as shown in Fig. 4, c. As a result, the effect of tightening the grippers along the lateral surfaces of the specimen ends will be achieved, that is, it will become pinched between the two grippers, as required by the procedure for performing experiments on flat composite specimens.

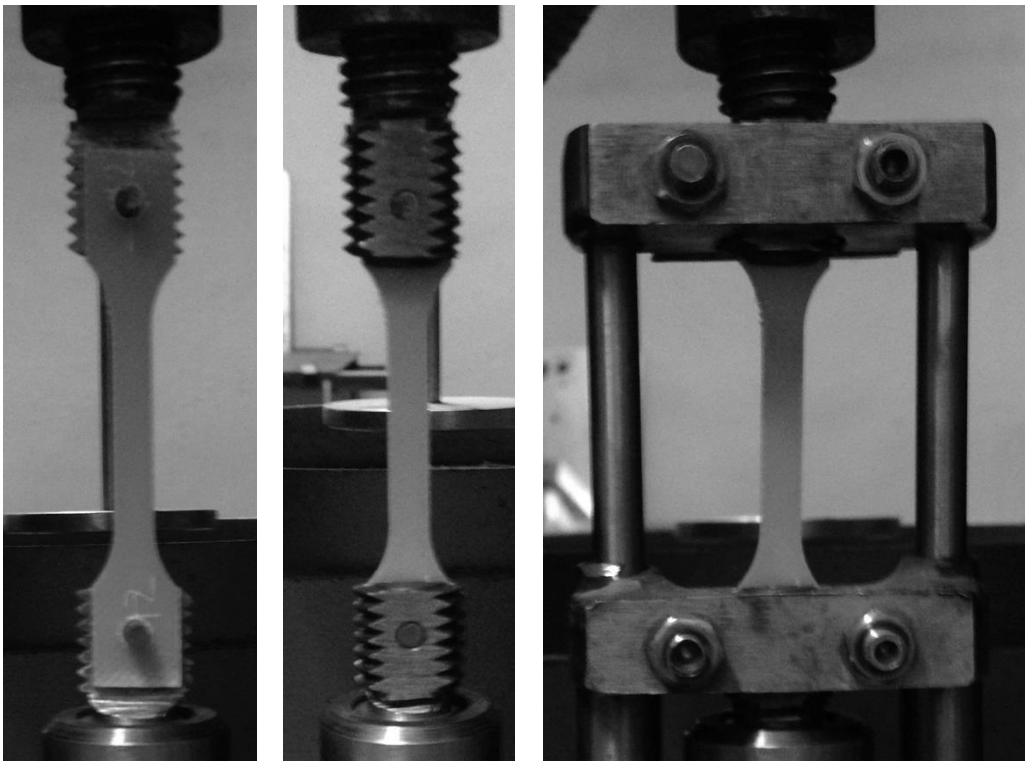

a b c

***Fig. 4. Process of installing specimens in the modernized gripper:***
a – first stage; b – second stage; c – third stage

**4. Automatic temperature control block for the electric furnace**

The automatic temperature control block for the electric furnace (ATCBEF), whose general view is shown in Fig. 5, is designed according to the structural scheme shown in Fig. 6.

As temperature sensors, semiconductor thermistors with a negative temperature coefficient of resistance (TCR) are used in the automatic control block. The reason for refusing to use traditional temperature sensors with bimetallic plates was both their low accuracy of operation and significant inertia as temperature regulators within the given operating temperature range of 75°C÷125°C.

The operation of the ATCBEF is carried out by the method of two-position regulation of the average power of the electric furnace, which is necessary in order to maintain the preset temperature in its working chamber. Under the experimental conditions, the insensitivity zone is set at ±0.5°C. The width of this zone is due to the


*Fig. 5. General view of the ATCBEF*

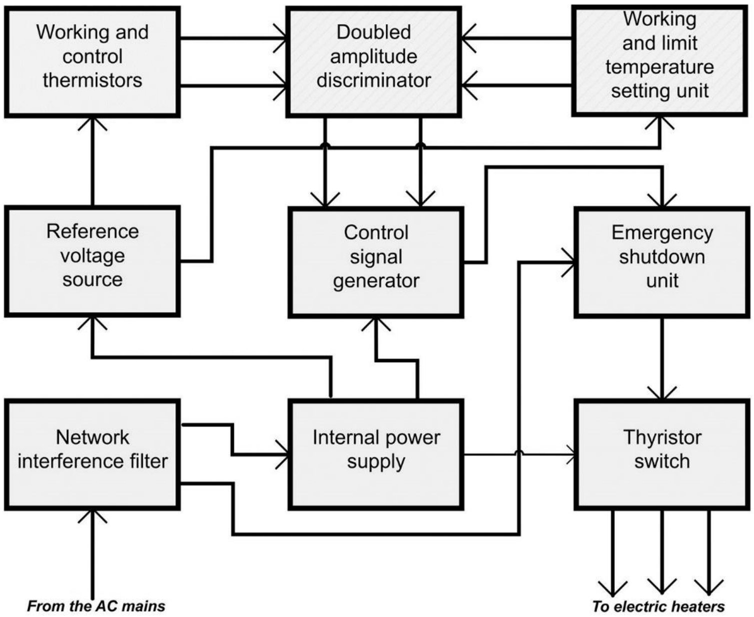


*Fig. 6. Structural scheme of the ATCBEF*

dynamic delay of semiconductor temperature sensors introduced by their metal protective covers filled inside with a non-conductive thermal paste, as well as by their tubular metal holders. The time lag is about 25 seconds.

The main measuring element of the automatic temperature control block is a dual amplitude discriminator implemented on an LM-311 integral comparator. Comparators switch the values of the output voltage depending on the input signals exceeding the preset levels. There are two such levels in the automatic control block:

− the operating temperature level of the electric furnace;

− the limit temperature level of the electric furnace.

These levels are formed under the influence of the temperature field by the operating and limiting measuring bridges, respectively, due to the thermistors included in them. The preliminary balancing of the measuring bridges connected to the comparator inputs is used to set the working and limiting temperatures of the electric furnace.

Connected to the output of the dual amplitude discriminator, the control signal conditioning block (CSCB) is essentially a logical device that implements the logical OR-NOT operation with a negative result. Thus, in a hardware implementation, the output signal of the CSCB, that opens the thyristor switch block (TSB), is formed if the set temperature threshold is not exceeded in relation to either the operating or limiting temperature. A similar control function is performed by the emergency shutdown unit (ESU) blocking the passage of the start signal to the TSB in the event of receiving a command signal from the magnetically controlled overload sensor located in the network interference filter unit (NIFU).

In addition, it should be noted that in order to reduce the value of the oscillations of the operating temperature of the automatic control block and shorten the time for the initial start-up, a stepwise switching mode of the electric furnace heating element is realized. So, immediately after the ATCBEF is switched on, all three parts of the heating element connected in parallel to the single-phase AC 220V network are involved in the operation. After the operating temperature of the electric furnace reaches the set value and after it is turned off by the CSCB signal, the TCB transfers the three parts of the heating element to the serial power mode, which does not change until the next restart of the entire ATCBEF.

To ensure the stable uninterrupted operation of the ATCBEF under the influence of various types of interference over the AC mains power supply network, the NIFU is included into the ATCBEF. The electrical circuit of this filter includes passive inductive and capacitive elements in the form of chokers with counter and cumulative winding, high-voltage non-polar capacitors, as well as a voltage surge limiter – a varistor. The two-stage interference filter built on the inductive and capacitive elements provides suppression of high-frequency in-phase network interferences at the level of 96 dB and the limitation of single voltage surges over 240 V. In addition, for an organization of a high-speed protection of the ATCBEF against overload and short circuits, the NIFU circuit has an X791151 chip-based magnetically controlled electronic switch, the chip output being connected to the second input of the ESU, as shown in Fig. 6.

The main technical characteristics of the developed and created ATCBEF designed for experimental studies of the strength characteristics of laminated fiberglass specimens, are given below.

| | |
|---|---|
| − Mean power consumption | 10 W |
| − Supply voltage of the unit | 220 V |
| − Maximum power of the electric furnace (in the primary heating mode) | 3.9 kW |
| − Electric furnace power in the operating mode | 1.3 кW |
| − Operating voltage of the electric furnace | 100 V |
| − Range of maintained temperatures in the electric furnace | 70÷130°C |
| − Time interval for entering the operating mode | 15÷20°min. |
| − Amplitude of temperature pulsations in the electric furnace | ±0.2°C |
| − Limiting temperature of the electric furnace | 150°C |
| − Threshold load current value of the unit (in the emergency mode) | 20 A |

**5. Procedure for conducting the experimental investigation**

The procedure and details of a series of experiments was planned according to the ASTM standards [29–31].

The specimens were cut out from a 2 mm thick single composite plate in the directions of 0°, 45° and 90°, which is shown in Fig. 2, *a*. They were loaded in the direction of their long side. Depending on the cutting direction, the process resulted in one of the three states, shown in Fig. 7.

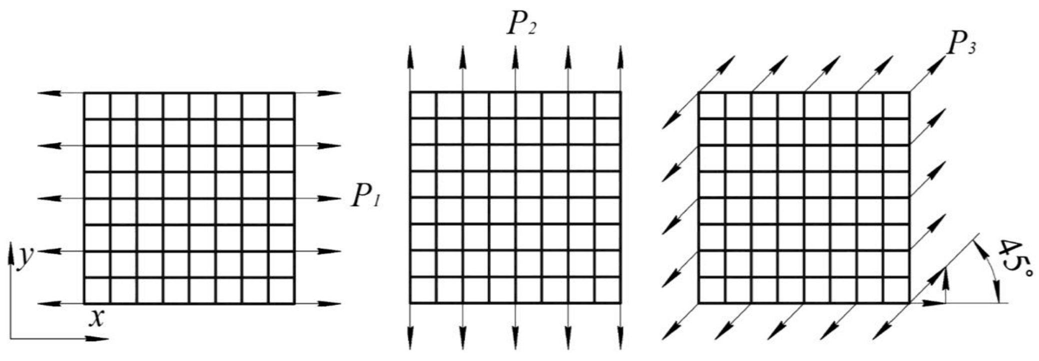


***Fig. 7. Scheme of specimen loading***

Such loading schemes allowed obtaining the planar mechanical properties of the composite material. Determination of the mechanical properties in the third direction (at right angles to the plane of a plate) requires tensile or compressive tests in these directions, which is difficult to implement. However, while modelling the mechanical behavior of thin composite plates and shells subjected to tensile and bending forces, there is only a need in the planar properties.

Fig. 8 shows the general view of the experimental installation. The specimen I is fixed in the grippers II while the heating element (the electric furnace) III is positioned around it. The relative displacement of the grippers is measured by two indicating gauges IV, and the temperature constancy is controlled by the sensor V. The heating element provides a smooth rise of the temperature up to 100°C maintaining it within the range of no more than ±2°C, as required in the ASTM standard D2990 [30].

To check the specimens for the correctness of pinching, they were loaded until their fracture, as shown in Fig. 9 for the specimens cut out at the angles of 0° and 45° to the first reinforcement direction, respectively. As can be seen from figs. 9, a and 9, b, the fracture occurs in the working part of the specimens, which indicates the effectiveness of the developed grippers.

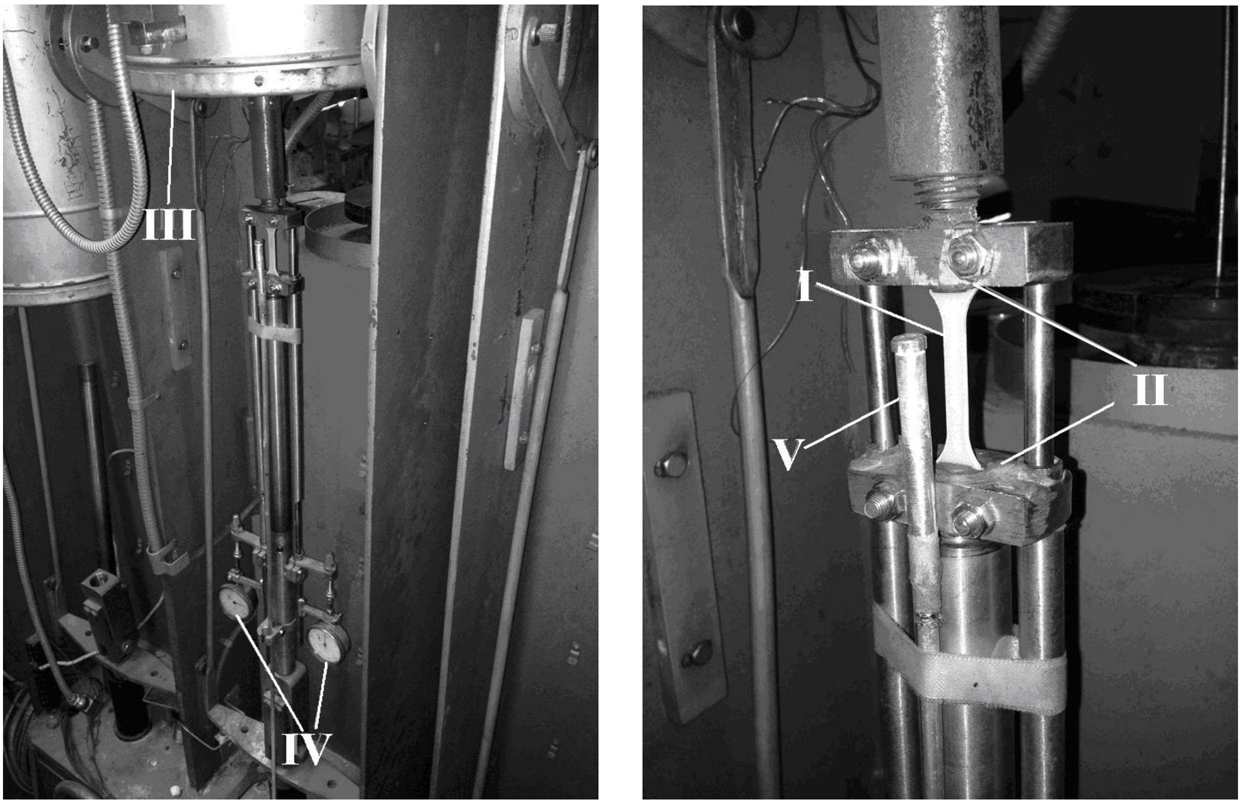


a b

***Fig. 8. Experimental installation:***
a) – general view; b) – view of the grippers

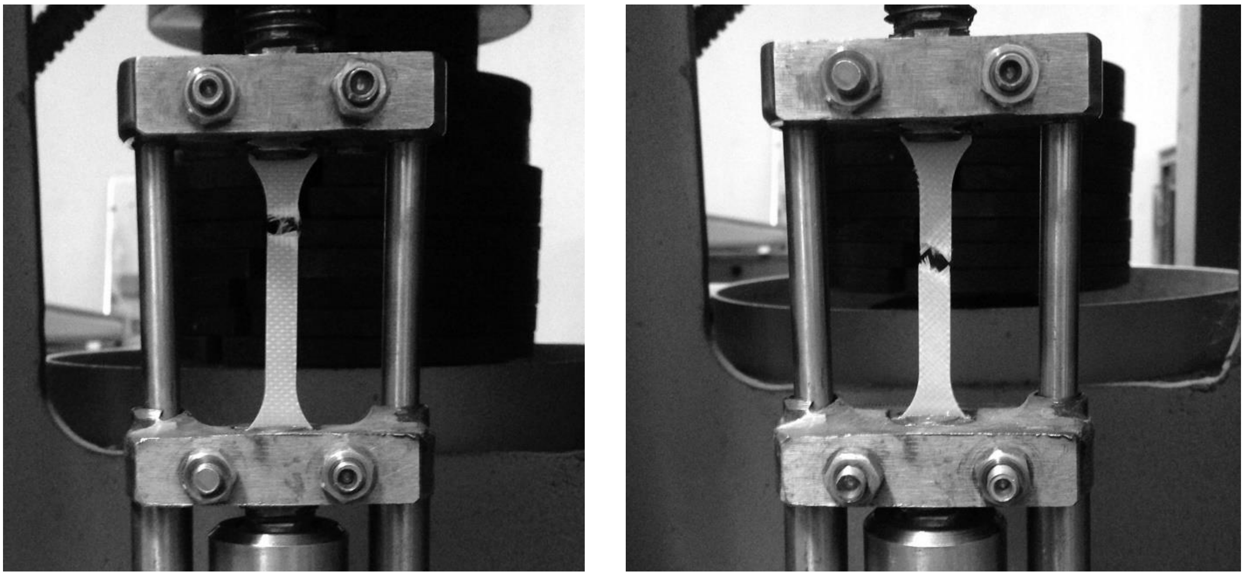

a b

***Fig. 9. Fracture of the specimens:***
a – specimen cut out at the angle of 0° to the fiber orientation;
b – specimen cut out at the angle of 45° to the fiber orientation

As a result of the experimental studies, the required graphs were built (Fig. 10): the stress-strain diagrams in different directions (Fig. 10, a) and the creep curves for different load levels (Fig. 10, b).

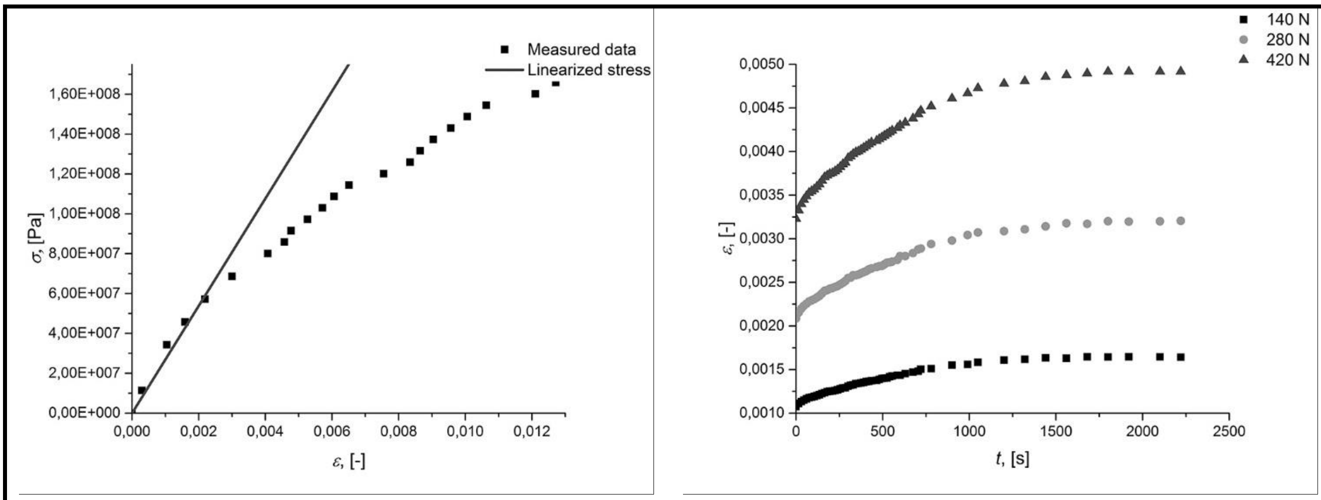


a b

***Fig. 10. Diagrams built using the experimental installation:***
a) – stress-strain diagram; b) – creep curves

After carrying out a series of experiments, it was established that the obtained results were highly repeatable, they were adequate for the specific effects of the considered ATCBEF, and the developed experimental technique was applicable to determining the mechanical properties of other ATCBEF types due to a sufficient range of possible loads applied to the specimens by means of the experimental installation and the temperatures realized with the help of the modernized electric heater.

## Conclusion

As a result of modernization, the experimental installation was adapted to perform studies of the high-temperature viscoelasticity of planar composite specimens. The modified grippers ensured the effective fastening of the specimens, which was confirmed by the experiments on their rupture. The developed ATCBEF, owing to the ability to maintain a constant temperature within the range of ±0.5°C allowed meeting the requirements of standards for maintaining the temperature regime when studying the mechanical properties of composite materials. The cut out specimens ensured a sufficiently accurate determination of the working part deformations, as a result of which the stress-strain and creep diagrams of the ATCBEF were built.

## References

1. Lubin G. (Ed.) Spravochnik po kompozitsionnym materialam [Handbook of Composite Materials]. Moscow: Mashinostroyeniye, 1988. 448 p.
2. Karpinos D. M. Kompozitsionnye materialy. Spravochnik [Composite Materials. Directory]. Kyiv: Naukova dumka, 1985. 588 p.
3. Kravchuk A. S., Mayboroda V. P. & Urzhumtsev Yu. S. Mekhanika polimernykh i kompozitsionnykh materialov [Mechanics of Polymer and Composite Materials]. Moscow: Nauka, 1985. 304 p.
4. Kapitonov A. M & Redkin V. Ye. Fiziko-mekhanicheskie svoystva kompozitsionnykh materialov [Physico-Mechanical Properties of Composite Materials. Elastic Properties]. Krasnoyarsk: Siberian Federal University Publ., 2013. 532 p.
5. Poberdrya B. Ye. Mekhanika kompozitsionnykh materialov [Mechanics of Composite Materials]. Moscow: Moscow University Publ., 1984. 336 p.
6. Ward I. Mekhanicheskie svoystva tverdykh polimerov [Mechanical Properties of Solid Polymers]. Moscow: Khimiya, 1975. 357 p.
7. Shen M. Vyazkouprugaya relaksatsiya v polimerakh [Viscoelastic Relaxation in Polymers]. Moscow: Mir, 1974. 270 p.
8. Christensen R. M. Introduction to the Theory of Viscoelasticity. Moscow: Mir, 1974. 338 p.
9. Adamov A. A. & Matveenko V. P. Vvedenie v teoriyu vyazkouprugosti [Methods of Applied Viscoelasticity]. Ekaterinburg: UB RAS Publ., 2003. 411 p.

10. Abot J., Yasmin A. & Jacobsen A. In-Plane Mechanical, Thermal and Viscoelastic Properties of a Satin Fabric Carbon/Epoxy Composite. Compos. Sci. Technol. 2004. Vol. 64. P. 263–268. doi: https://doi.org/10.1016/S0266-3538(03)00279-3
11. Chan A., Liu X. L. & Chiu W. K. Viscoelastic Interlaminar Shear Modulus of Fibre Reinforced Composites. Compos. Struct. 2006. Vol. 75. P. 185–191. doi: https://doi.org/10.1016/j.compstruct.2006.04.058
12. Guojun H. A Theoretical and Numerical Study of Crack Propagation Along a Bimaterial Interface with Applications to IC Packaging: a thesis … doctor of philosophy in engineering (Doctor thesis). National University of Singapore. 2006.
13. Silva P., Valente T. & Azenha M. Viscoelastic Response of an Epoxy Adhesive for Construction Since Its Early Ages: Experiments and Modelling. Compos. Part B Eng. 2017. Vol. 116. P. 266–277. doi: https://doi.org/10.1016/j.compositesb.2016.10.047
14. Seifert O. E., Schumacher S. C. & Hansen A. C.. Viscoelastic Properties of a Glass Fabric Composite at Elevated Temperatures: Experimental and Numerical Results. Compos. Part B. Eng. 2003. Vol. 34. P. 571–586. doi: https://doi.org/10.1016/S1359-8368(03)00078-7
15. Ciambella J., Paolone A. & Vidoli S. A comparison of Nonlinear Integral-Based Viscoelastic Models Through Compression Tests on Filled Rubber. Mech. Mater. 2010. Vol. 42. P. 932–944. doi: https://doi.org/10.1016/j.mechmat.2010.07.007
16. Stanier D. C., Patil A. J. & Sriwong C. The reinforcement Effect of Exfoliated Graphene Oxide Nanoplatelets on the Mechanical and Viscoelastic Properties of Natural Rubber. Compos. Sci. Technol. 2014. Vol. 95. P. 59–66. doi: https://doi.org/10.1016/j.compscitech.2014.02.007
17. Shrotriya P. & Sottos N. Viscoelastic Response of Woven Composite Substrates. Compos. Sci. Technol. 2004. Vol. 65. P. 621–634. doi: https://doi.org/10.1016/j.compscitech.2004.09.002
18. Park S. J., Liechti K. M. & Roy S. Simplified Bulk Experiments and Hygrothermal Nonlinear Viscoelasticity. Mech. Time-Dependent Mater. 2004. Vol. 8. P. 303–344. doi: https://doi.org/10.1007/s11043-004-0942-3.
19. Tzeng J. T., Emerson R. P. & O'Brien D. J. Viscoelasticity Analysis and Experimental Validation of Anisotropic Composite Overwrap Cylinders. Mech. Solids, Struct. Fluids, ASME. 2012. Vol. 8. P. 1–8. doi: https://doi.org/10.1115/IMECE2012-87818
20. Kluev V. Ispytatelnaya tekhnika: Spravochnik [Testing Equipment: Hanbook]. Moscow: Mashinostroyeniye, 1982. 560 p. (in Russian).
21. Sathishkumar T., Satheeshkumar S. & Naveen J. Glass Fiber-Reinforced Polymer Composites – A review. J. Reinf. Plast. Compos. 2014. Vol. 33. P. 1258–1275. doi: https://doi.org/10.1177/0731684414530790
22. Stickel J. M. & Nagarajan M. Glass Fiber-Reinforced Composites: From Formulation to Application. Int. J. Appl. Glas. Sci. 2012. Vol. 3. P. 122–136. doi: https://doi.org/10.1111/j.2041-1294.2012.00090.x
23. Yamini S. & Young R. J. The mechanical Properties of Epoxy Resins. J. Mater. Sci. 1980. Vol. 15**.** P. 1823–1831. doi: https://doi.org/10.1007/BF00550603
24. Jordan J. L. & Foley J. L. Mechanical Properties of Epon 826/DEA Epoxy. Mech. Time-Dependent Mater. 2008. Vol. 12. P. 249–272. doi: https://doi.org/10.1007/s11043-008-9061-x
25. Ou Y., Zhu D., Zhang H., Huang L., Yao Y. & Li G. Mechanical Characterization of the Tensile Properties of Glass Fiber and Its Reinforced Polymer (GFRP) Composite Under Varying Strain Rates and Temperatures. Polymers. 2016. Vol. 8. P. 1–16. doi: https://doi.org/10.3390/polym8050196
26. Dogan A. & Atas C. Variation of the Mechanical properties of E-Glass/Epoxy Composites Subjected to Hygrothermal Aging. J. Compos. Mater. 2016. Vol. 50. P. 637–646. doi: https://doi.org/10.1177/0021998315580451
27. Ferry J. D. Viscoelastic Properties of Polymers. John Wiley & Sons. 1980. 641 p.
28. ASTM D618-13 Standard Practice for Conditioning Plastics for Testing. Am. Soc. Test. Mater. 2013. 08. 01. doi: https://doi.org/10.1520/D0618
29. ASTM D638-14. Standard Test Method for Tensile Properties of Plastics. Am. Soc. Test. Mater. 2014. 08. 01. doi: https://doi.org/10.1520/D0638-14
30. ASTM D2990-17. Standard Test Methods for Tensile, Compressive, and Flexural Creep and Creep-Rupture of Plastics. Am. Soc. Test. Mater. 2017. 08. 01. doi: https://doi.org/10.1520/D2990-17
31. ASTM D3039/D3039M-17 Standard Test Method for Tensile Properties of Polymer Matrix Composite Materials. Am. Soc. Test. Mater. 2017. 15. 03. doi: https://doi.org/10.1520/D3039_D3039M-17

*Received 17 January 2018*